

# Biobased Polyurethanes Prepared from Different Vegetable Oils

Chaoqun Zhang,<sup>†</sup> Samy A. Madbouly,<sup>†,§</sup> and Michael R. Kessler<sup>\*,†,‡</sup>

<sup>†</sup>Department of Materials Science and Engineering, Iowa State University, Ames, Iowa, United States

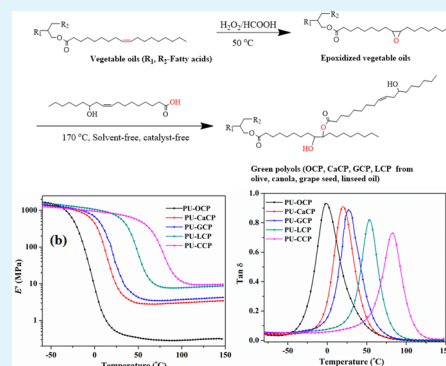
<sup>‡</sup>School of Mechanical and Materials Engineering, Washington State University, Pullman, Washington, United States

<sup>§</sup>Department of Chemistry, Faculty of Science, Cairo University, Orman-Giza, Egypt

## Supporting Information

**ABSTRACT:** In this study, a series of biobased polyols were prepared from olive, canola, grape seed, linseed, and castor oil using a novel, solvent/catalyst-free synthetic method. The biobased triglyceride oils were first oxidized into epoxidized vegetable oils with formic acid and hydrogen peroxide, followed by ring-opening reaction with castor oil fatty acid. The molecular structures of the polyols and the resulting polyurethane were characterized. The effects of cross-linking density and the structures of polyols on the thermal, mechanical, and shape memory properties of the polyurethanes were also investigated.

**KEYWORDS:** vegetable oil, polyol, polyurethane, shape memory



## 1. INTRODUCTION

Polyurethanes (PUs), prepared via a polyaddition reaction between a diisocyanate and a polyol, are widely used in applications such as coatings, adhesives, sealants, and foams because of their excellent abrasion resistance, high toughness, chemical resistance, and low film-forming temperatures.<sup>1–3</sup> The global market for PUs was estimated at 14 million tons in 2010, and is expected to increase by 28% by 2016.<sup>4</sup> Over the past decades, most of the starting materials for the production of PUs are derived from petroleum-based resources, which are widely regarded as unsustainable. Recently, environmental concerns, the depletion of the world crude oil stock and the increasing price of crude oil have triggered increasing interest to utilize biobased resources for the production of PUs.<sup>5,6</sup>

Several biobased materials, including cellulose, starch, natural oil, and sugar, have been utilized as starting materials for PUs.<sup>7–10</sup> Vegetable oils are among the most promising, because they are an inexpensive, readily available, and renewable resource. Vegetable oils are triglycerides of saturated and unsaturated fatty acids. The six most common fatty acids are palmitic (C16:0), stearic (C 18:0), oleic (C 18:1), linoleic (C 18:2), linolenic (C 18:3), and ricinoleic (C18:1 OH) acids (in this notation, the first number represents the number of carbon atoms, the second number represents the number of carbon–carbon double bonds, and OH represents hydroxyl groups in the fatty acid). In order to utilize vegetable oils for PU applications, a variety of techniques are used to introduce hydroxyl groups into the fatty acid chains at the position of carbon–carbon double bonds, thus creating polyols.

Epoxidation of vegetable oils, followed by oxirane ring opening is one of the most important reactions to provide various polyols. Different ring-opening chemical agents, such as H<sub>2</sub>,<sup>11</sup> hydrohalic acids,<sup>11</sup> organic acids,<sup>12</sup> and amines,<sup>13</sup> are typically used to initiate the ring opening reaction; they create polyols with different functionalities for PUs that exhibit a broad range of properties, from soft and rubbery to hard and glassy. However, almost all ring opening agents used to prepare polyols by ring-opening of epoxidized vegetable oils are petroleum-based, small molecules. Currently, several research groups dedicate considerable effort to the development of 100% biopolyols for the production of PUs. Kiatsimkul<sup>14</sup> initiated ring-opening reactions of epoxidized soybean oil with linoleic acid, ricinoleic acid, and ricinoleic acid estolide to prepare high hydroxyl equivalent weight polyols. Recently, polyols were developed by ring-opening reactions between epoxidized soybean oil and castor oil fatty acid (COFA) using a solvent method without catalyst.<sup>15</sup>

The mechanical and physical properties of PUs strongly depend on the types of polyol used (the number and distribution of hydroxyl groups), the diisocyanate, and the diisocyanate index. Lu et al. investigated the effect of different OH functionalities of soy-methanol polyols on the thermo-physical and mechanical properties of waterborne PU films.<sup>16</sup> Petrovic et al. reported the effect of OH/NCO molar ratios on the physical, thermal and mechanical properties of soy-

Received: October 15, 2014

Accepted: December 26, 2014

Published: December 26, 2014

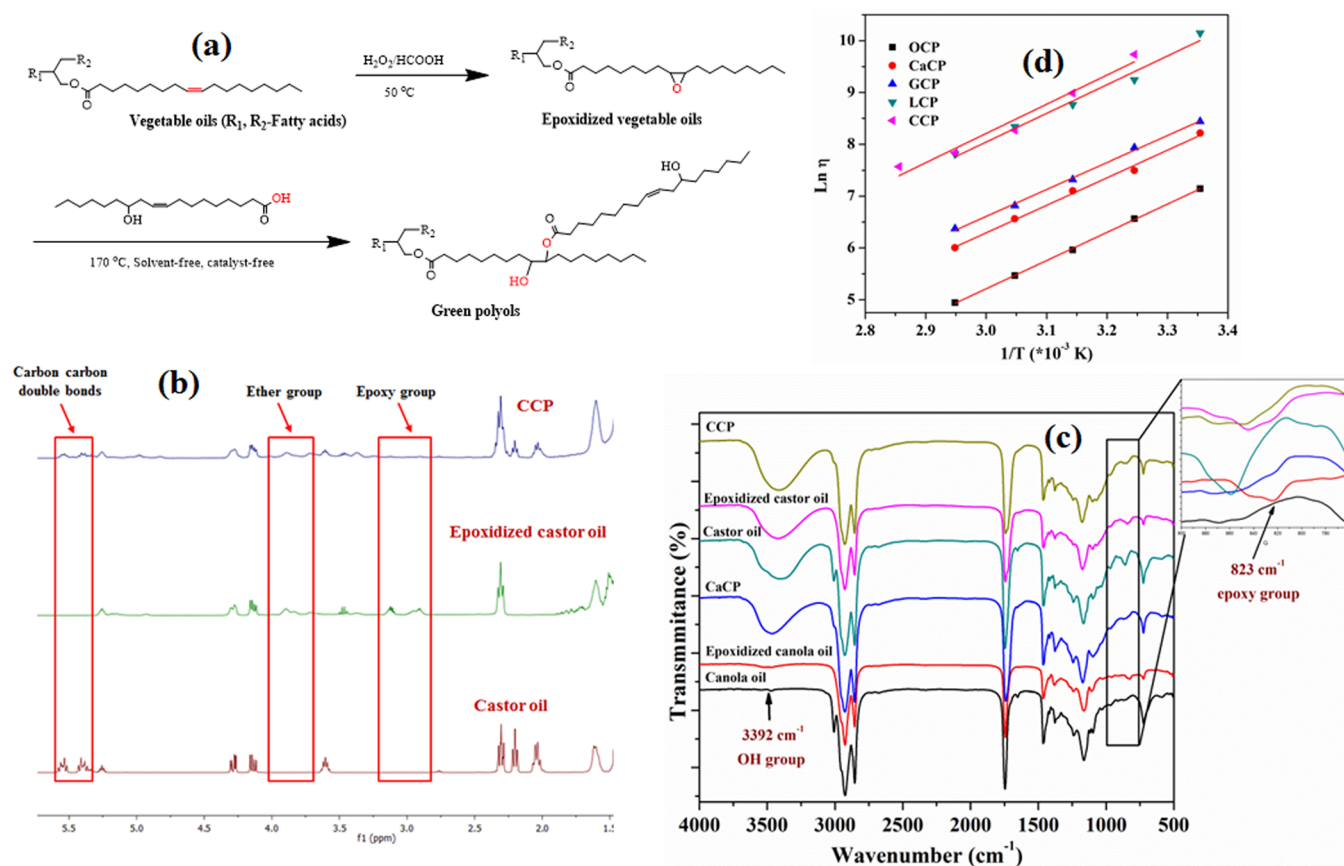


**Figure 1.** (a) Preparation of vegetable oil-based polyols; (b) <sup>1</sup>H NMR spectra of castor oil, epoxidized castor oil, and CCP; (c) FTIR spectra of CCP, epoxidized castor oil, castor oil, CaCP, epoxidized canola oil, and canola oil; (d) viscosity-temperature relationship for OCP, CaCP, GCP, LCP, and CCP.

methanol-PU.<sup>17</sup> Peruzzo et al. studied the effect of different diisocyanates structures on the morphology and properties of waterborne PU-acrylates.<sup>18</sup> It was reported that soy–castor oil-based polyol prepared using a solvent/catalyst-free method resulted in PUs with better thermophysical and mechanical properties than those from soy–methanol polyols and castor oil-based polyols because of the pre-cross-linking structures of soy–castor oil-based polyol.<sup>15</sup>

Shape memory is an important property for many polymers that are stimuli-responsive (temperature, light, solvent), i.e., have the ability to return from a deformed (temporary) state to their original, primary shape when an external trigger is applied. Numerous PUs exhibit shape memory properties.<sup>19</sup> The shape memory properties of PUs from those synthesized from 100% biobased polyols using a solvent/catalyst-free method have not been determined.

In this study, a solvent/catalyst-free method is described to prepare a series of vegetable oil-based polyols from olive, canola, grape seed, linseed, and castor oils. The properties of these polyols are characterized by proton nuclear magnetic resonance (<sup>1</sup>H NMR), Fourier transform infrared spectroscopy (FTIR), gel permeation chromatography (GPC), and rheology. In addition, PUs prepared from these polyols and IPDI are described. The properties of the PUs are characterized by dynamic mechanical analysis (DMA), differential scanning calorimetry (DSC), thermogravimetric analysis (TGA), and tensile strength tests. The effect of cross-link density and structure of the polyols from different vegetable oils on the

thermo-mechanical, thermal resistance, and shape memory properties of the PUs are investigated.

## 2. MATERIALS AND METHODS

**2.1. Materials.** Epoxidized linseed oil (approximately 6 oxirane rings per triglyceride) was purchased from Scientific Polymer Inc., New York, NY. Magnesium sulfate (MgSO<sub>4</sub>), hydrogen peroxide, methyl ethyl ketone (MEK), and ethyl ether were purchased from Fisher Scientific Company (Fair Lawn, NJ). Olive oil, canola oil, castor oil, grape seed oil, hydrochloric acid, sodium hydroxide, sodium bicarbonate, formic acid, isophorone diisocyanate (IPDI), and dibutyltin dilaurate (DBTDL) were obtained from Sigma-Aldrich (Milwaukee, WI). All materials were used as received without further purification.

**2.2. Synthesis of the Epoxidized Vegetable Oils.** Epoxidized vegetable oils with different epoxy groups were prepared according to a method previously reported.<sup>20</sup> Briefly, vegetable oils and formic acid (the molar ratio of these two is 1:4.12) were charged into a 500 mL flask at 50 °C under vigorous stirring. Then, hydrogen peroxide (50%, the molar ratio of hydrogen peroxide to double bonds in triglyceride is 1.8:1) was added slowly using syringe over a 4 h period (The addition of hydrogen peroxide should be conducted carefully and slowly to avoid any safety issue). The reaction was continued at 50 °C for another 4 h. Then, sodium bicarbonate was added to neutralize the solution and ethyl ether was added, resulting in two layers. The organic layer was washed with distilled water until the solution became neutral. Epoxidized vegetable oils were obtained after drying with MgSO<sub>4</sub> and filtering, removal of organic solvent by rotary evaporation, and drying in a vacuum oven overnight.

**2.3. Synthesis of Castor Oil Fatty Acid.** Castor oil was saponified into fatty acid with a sodium hydroxide solution at 80

Table 1. Properties of the OCP, CaCP, GCP, LCP, and CCP<sup>a</sup>

		C=C bonds	epoxy	OH number (mg KOH/g)	number/average molecular weight	PDI	state at room temperature
#1	OO	2.48	0		1295/1327	1.03	liquid
	E-OO	0	2.47		1333/1366	1.02	liquid
	OCP			109.1 ± 0.1	2118/2675	1.26	liquid
#2	CaO	3.54	0		1305/1358	1.04	liquid
	E-CaO	0	3.29		1371/1425	1.04	liquid
	CaCP			132.7 ± 0.4	2419/3380	1.4	liquid
#3	CO	2.94	0		1391/1461	1.05	liquid
	E-CO	0.24	1.9		1862/2217	1.19	wax
	CCP			227.9 ± 0.5	2553/3581	1.4	wax
#4	GO	4.17	0		1392/1435	1.03	liquid
	E-GO	0	4.17		1530/1620	1.06	liquid
	GCP			140.1 ± 0.9	2624/3546	1.35	liquid
#5	E-LO	0	6.00		1337/1590	1.19	liquid
	LCP			173.2 ± 3	2842/4827	1.7	liquid

<sup>a</sup>OO, olive oil; CaO, canola oil; CO, castor oil; GO, grape seed oil; LO, linseed oil; E, epoxidized; PDI, polydispersity index.

°C, followed by neutralization with hydrochloric acid.<sup>15</sup> Finally, castor oil fatty acids-COFA, which consist of 87.7–90.4% ricinoleic acid, the rest are linolenic, linoleic, and oleic acid,<sup>21,22</sup> were obtained after the organic layer was purified by washing with water, drying over MgSO<sub>4</sub>, and filtering.

**2.4. Synthesis of Vegetable Oil-Based Polyols.** The polyols were prepared by ring-opening reactions between epoxidized vegetable oils and COFA. The polyols were identified as olive–castor oil-based polyols (OCP), canola–castor oil-based polyols (CaCP), castor–castor oil-based polyols (CCP), grape seed–castor oil-based polyols (GCP), and linseed–castor oil-based polyols (LCP). Initially, COFA and epoxidized vegetable oil were mixed in a flask with a magnetic stirrer and maintained at 170 °C in dry nitrogen atmosphere. The molar ratio of the carboxyl to the epoxy groups was 0.5. After 8 h, a viscous liquid was obtained.

**2.5. Polyurethane Preparation.** The PUs were synthesized through the reaction of polyol with a 5% molar excess of IPDI in the presence of DBTDL. The viscosity of the mixture was reduced by the use of MEK. The solution was heated to 70 °C and mixed continuously for 3 h. Then, the mixture was poured into a Teflon mold to produce 50 mm × 50 mm (length × width) sheets, which were dried overnight in an oven at 80 °C. Finally, the PU films were cut into specific dimensions for thermo-mechanical tests.

**2.6. Characterization.** A Varian spectrometer (Palo Alto, CA) at 300 MHz was used to record the <sup>1</sup>H NMR spectroscopic analyses of the monomers and final products. All measurements were carried out using CDCl<sub>3</sub> as solvent. The FTIR spectra of the polyols were recorded on a Nicolet 460 FTIR spectrometer (Madison, WI). The OH number of polyols were determined using the Unilever method.<sup>11</sup> The acid numbers of the polyols were determined by AOCS Official Method Te 1a-64. The molecular weight was determined using a THF-eluted GPC equipped with a refractive index detector. Thermal and mechanical properties of the resulting PU films were characterized using a TA Instruments Q800 dynamic mechanical analyzer with a film-tension mode at 1 Hz. Rectangular specimens of 0.6 × 10 mm (thickness × width) were used for the analysis. The samples were cooled and held isothermally for 2 min at –80 °C before the temperature was increased to 150 °C at a heating rate of 3 °C/min. A TA Instrument Q2000 differential scanning calorimeter was used to examine the glass transition temperature (*T*<sub>g</sub>). Approximately 6 mg of each PU sample was heated in a first cycle from room temperature to 120 °C at a rate of 20 °C/min to erase their thermal history. Then the samples were equilibrated at –60 °C and heated for a second cycle to 120 °C at a heating rate of 20 °C/min. TGA was carried out using a TA Instrument Q50 to evaluate the thermal stability of the PU films. Samples with a weight of approximately 10 mg were heated from room temperature to 700 °C at a heating rate of 20 °C/min in air. An Instron universal testing machine (model 4502) with a crosshead speed of 100 mm/min was used to determine the tensile properties of

the PU films; rectangular specimens of 50 mm × 10 mm (length × width) were used. Average values of at least four replicates of each sample were taken. The toughness of the PU samples was determined from the area under the corresponding tensile stress/strain curves.

Shape memory properties of the PUs were investigated using a TA Instruments Q800 dynamic mechanical analyzer. The samples were equilibrated at *T*<sub>prog</sub> and held for 2 min, then stretched to the maximum strain ( $\epsilon_m$ ) at a rate of 10% /min. While maintaining the stress applied, the samples were cooled down to *T*<sub>low</sub> at 10 °C/min and held at this temperature for 10 min. Then the stress was released and the sample was held for another 2 min to reach a predetermined strain ( $\epsilon_u$ ). Finally, the temperature was increased to *T*<sub>high</sub> at a rate of 3 °C/min and held at this temperature for 30 min to recover a fixed strain ( $\epsilon_p$ ). The values of *T*<sub>prog</sub>, *T*<sub>low</sub>, *T*<sub>high</sub> based on the different *T*<sub>g</sub> values of the samples will be discussed later. The PU-GCP samples underwent four consecutive cycles.

### 3. RESULTS AND DISCUSSION

**3.1. Structures and Properties of Polyols.** Figure 1a shows the pathway for the preparation of green polyols. <sup>1</sup>H NMR spectra of castor oil, epoxidized castor oil, and the castor–castor oil-based polyol are shown in Figure 1 (b). The area under the peaks at 4.1–4.2 ppm (–CH<sub>2</sub>–CHCH<sub>2</sub>–) was used as a constant of 2 for normalization to obtain the number of carbon–carbon double bonds and epoxy groups in the structure of the vegetable oils and epoxidized vegetable oils, see Table 1. Figure 1 (b) shows that after epoxidation, the carbon–carbon double bonds (peaks between 5.3 and 5.6 ppm) in castor oil disappeared and epoxy groups (peaks between 2.8 and 3.2 ppm in spectra of epoxidized castor oil) were formed. As seen in Table 1, the conversion ratios of double bonds to epoxy groups (number of epoxy groups in epoxidized vegetable oils/number difference of carbon–carbon double bonds between epoxidized vegetable oils and vegetable oil) are only 70% while other vegetable oils are approximately 90%. This was attributed to the fact that the newly formed epoxy groups were ring opened by hydroxyl groups that originally existed in castor oil with formic acid as catalyst, seen in the decrease of peaks at 3.5–3.6 ppm corresponding the hydrogen attached to the carbon adjacent to OH in the spectra of castor oil and in the appearance of new peaks between 3.6 and 4.0 ppm that represent tertiary hydrogen atoms adjacent to the newly formed ether in the spectra of epoxidized castor oil. Subsequent to the ring opening reaction between epoxidized castor oil and COFA, the number of epoxy groups decreased. In addition, the



presence of new peaks between 4.6 and 5.0 ppm, representing tertiary hydrogen atoms adjacent to the newly formed ester groups, indicated that COFA (contains carbon–carbon double bonds) was attached to the long carbon chain of epoxidized oils. The reappearance of carbon–carbon double bond peaks in the spectra of CCP also confirmed this result. Similar results were found for other vegetable oil systems shown in Figure 1 in the Supporting Information.

The successful preparation of polyols was also confirmed by FTIR. Figure 1 (c) shows the FTIR spectra of CCP, epoxidized castor oil, castor oil, CaCP, epoxidized canola oil, and canola oil. After epoxidation from castor oil and canola oil, oxirane absorption at 823  $\text{cm}^{-1}$ , corresponding to epoxy groups appeared and carbon–carbon double bonds at 3000–3010  $\text{cm}^{-1}$  almost disappeared. After the ring opening reaction was initiated by COFA, the epoxy groups in epoxidized castor oil and epoxidized canola oil decreased, while a broad peak at 3392  $\text{cm}^{-1}$  appears in CaCP, which suggests that the epoxy groups in epoxidized castor and canola oil were ring-opened and hydroxyl groups were formed. Because castor oil originally contained OH groups, it exhibited a broad peak at 3392  $\text{cm}^{-1}$ , whereas canola oil did not exhibit this peak.

Table 1 shows that OCP, CaCP, GCP, and LCP were liquids at room temperature, whereas CCP was a waxy solid. LCP has highest molecular weight while OCP has lowest. Figure 1d shows the viscosity of OCP, CaCP, GCP, LCP, and CCP as a function of temperature. At 66 °C and a shear rate of 25  $\text{s}^{-1}$ , the viscosity of polyols increased from OCP < CaCP < GCP < LCP < CCP, see Table 2, because of the effect of hydrogen

**Table 2. Viscosity at 66 °C and the Activation Energy of the Viscous-Flow for Polyols**

	viscosity (Pa s) at 66 °C at a shear rate of 25 $\text{s}^{-1}$	$E_{ac}$ (kJ/mol)
OCP	0.14	45.3
CaCP	0.40	44.1
GCP	0.59	43.2
LCP	2.47	46.0
CCP	2.52	46.9
ESBO <sup>11</sup>	0.06 (70 °C)	35
castor oil <sup>11</sup>	0.09 (70 °C)	33

bonding and molecular weights. The number of carbon–carbon double bonds for vegetable oils increased from olive oil < castor oil < canola oil < grape seed oil, while the number of epoxy groups for epoxidized vegetable oils increased from epoxidized castor oil < epoxidized olive oil < epoxidized canola oil < epoxidized grape seed oil < epoxidized linseed oil. Among these five epoxidized vegetable oils, only epoxidized castor oil originally contained OH groups. Also, the ring opening of one epoxy group generated one OH group in all systems. Therefore, the OH numbers of the polyols increased from OCP < CaCP < GCP < LCP < CCP, see Table 1. The highest OH number in CCP generates the greatest hydrogen bonding, resulting in CCP a waxy state at room temperature. When plotted against the reciprocal temperature (Figure 1d), the viscosities obeyed the Andrade dependence.<sup>24</sup>

$$\eta = 3\eta_0 e^{E_{ac}/RT} \quad (1)$$

where  $\eta_0$  is a reference viscosity,  $E_{ac}$  is the viscous-flow activation energy,  $R$  is the universal gas constant and  $T$  is the temperature. The activation energies were calculated from the

slopes of the lines in Figure 1d and are summarized in Table 2. The activation energy of different polyols did not change significantly. However, the activation energies of the polyols were higher than those of ESBO and castor oil because of the effect of hydrogen bonding.

**3.2. Properties of PUs.** Figure 2a shows the DSC curves of the PUs from different polyols, and their  $T_g$  values are summarized in Table 3, which were determined from the midpoint temperature in the heat capacity change of the DSC scan. All PUs exhibited only one  $T_g$  and neither melting nor crystallization transitions were observed in the DSC curves, indicating the amorphous nature of these PUs. As the OH numbers increased from OCP, CaCP, GCP, LCP, to CCP, the  $T_g$  values increased from –22.9 to 54.55 °C, respectively, which was explained by the fact that urethane linking increased with increasing OH numbers, leading to higher cross-linking densities, that restricted the mobility of the polymer chains. Kong<sup>25</sup> and Javni<sup>26</sup> reported that as the OH numbers of vegetable oil-based polyols increased, the increasing amount of isocyanate necessary during PU preparation contained more rigid aliphatic rings, and resulted in higher  $T_g$  values.

The thermal and mechanical properties of the polymer phase were investigated by DMA. Figures 2b, c show the storage modulus and  $\tan \delta$  as functions of temperature ranging from –80 to 150 °C for PUs from different vegetable oils. The temperature corresponding to  $\tan \delta_{\max}$  is taken as the glass transition temperature ( $T_g$ ,  $\alpha$  relaxation). At low temperatures, all PU samples were in the glassy state with  $E'$  values on the order of 1000 MPa. As temperature increased,  $E'$  gradually decreased until a rapid decrease was observed. At higher temperatures, the storage moduli of all PUs reached a rubbery plateau. All samples show only one  $\tan \delta$  peak, indicating the homogeneous nature of the PU films. As the OH numbers of the polyols increased from OCP, CaCP, GCP, LCP to CCP, the  $\tan \delta$  peak of the respective PUs shifted to higher temperatures and their maxima decreased. This is attributed to the fact that increasing OH numbers caused higher cross-linking densities ( $\nu_c$ ) and thus less energy was dissipated throughout the polymers, see Table 3. The cross-linking densities of all films were determined from the rubbery moduli using the kinetic theory of rubber elasticity.<sup>27</sup>

$$E' = 3\nu_c RT' \quad (2)$$

where  $T'$  is the absolute temperature at  $T_g + 40$  °C, and  $E'$  is the storage modulus at  $T'$ .  $R$  is the gas constant.

Figure 2d shows that the  $T_g$  values exhibited linear behavior as functions of the polyols' OH number, which matches reports by Lu<sup>28</sup> and Petrovic et al.<sup>29</sup> The  $T_g$  values determined by DMA were approximately 20–30 °C higher than those determined by DSC because of the different principles underlying these two methods.<sup>30</sup>

TGA weight loss and weight loss derivative curves in air for PU films from different oils are shown in Figure 3a, b, respectively. The weight loss derivative curves of the PUs revealed that all films underwent three main degradation processes: The degradation between 200 and 340 °C was initiated by the decomposition of unstable urethane bonds, leading to primary or second amines, olefin, and dioxide.<sup>31,32</sup> As OH numbers of the polyols increased, the thermal stability of the corresponding PUs decreased because of the increasing urethane bonds. The weight loss in the temperature range from 340 to 500 °C corresponded to chain scission of the oils.<sup>28,33</sup> At this stage, there was no obvious trend, because with increasing

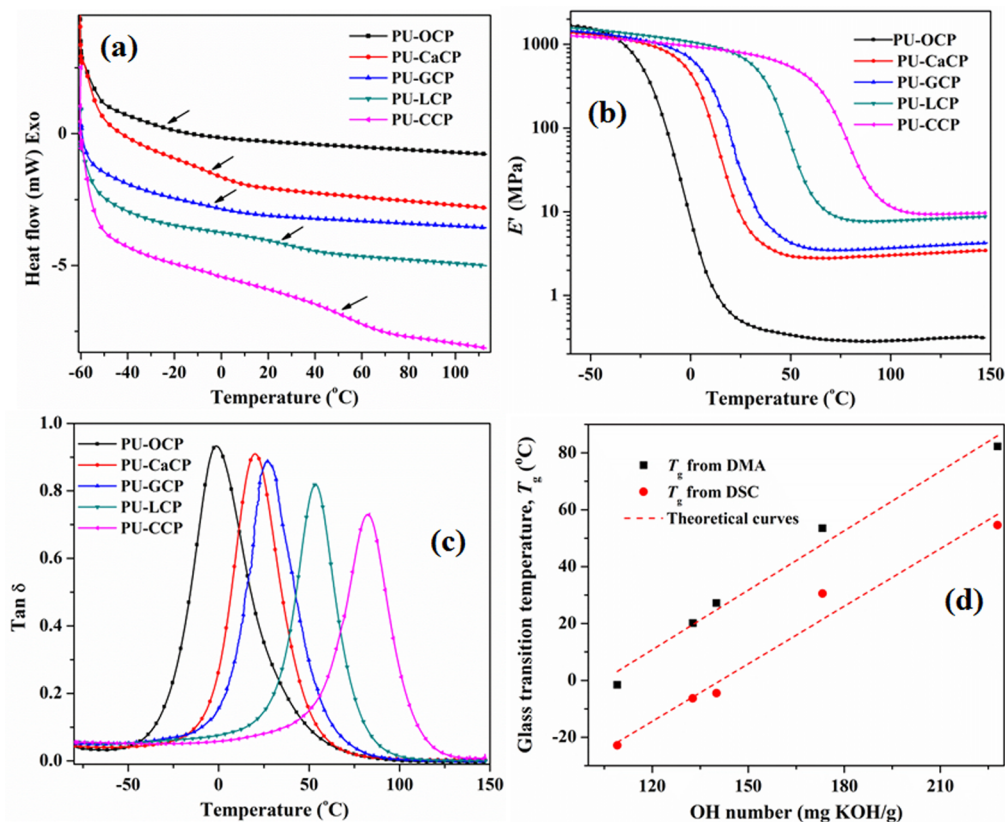


**Figure 2.** (a) DSC traces (20 °C/min), (b) temperature dependence of  $E'$ , and (c) temperature dependence of  $\tan \delta$  of PUs from OCP, CaCP, GCP, LCP, and CCP, (d) the dependence of  $T_g$  of PU films on the OH number of corresponding polyols.

**Table 3. Thermal Properties of PUs Based on Polyols from Different Vegetable Oils**

	DMA $T_g$ (°C)	DSC $T_g$ (°C)	$v_e$ (mol/m <sup>3</sup> )	$E'$ at 25 °C (MPa)	TGA in air (°C)	
					$T_{10}^a$	$T_{50}^b$
PU-OCP	-1.58	-22.9	48.8	0.5	310.3	378.3
PU-CaCP	20.11	-6.3	339.1	9.1	312.6	386.2
PU-GCP	27.2	-4.5	412.1	32.5	308.0	380.0
PU-LCP	53.46	30.5	841.8	713.4	311.6	377.7
PU-CCP	82.3	54.55	948.6	798.6	302.4	368.4

<sup>a</sup>10% weight loss temperature. <sup>b</sup>50% weight loss temperature.

OH numbers, the positive effect of the ester group (precross-linking) on the weight loss to some extent compensated for the negative effect of the urethane groups on the thermal stability of the PUs. The decomposition of PUs above 500 °C contributed to further thermo-oxidation of the PU films.

Figure 4 shows the representative stress–strain curves of PUs from different vegetable oils. Young's modulus, tensile strength, elongation at break, and toughness of PU films are summarized in Table 4. The PUs derived from OCP, CaCP, and GCP exhibited the elastic region and yield point of typical elastomeric polymers while PUs from linseed oil and castor oil exhibited the stress–strain behavior of hard plastics with followed by strain softening and strain hardening before breaking. As the OH number of the polyols increased, the tensile strength of the PUs increased. Except for PU-CCP, the

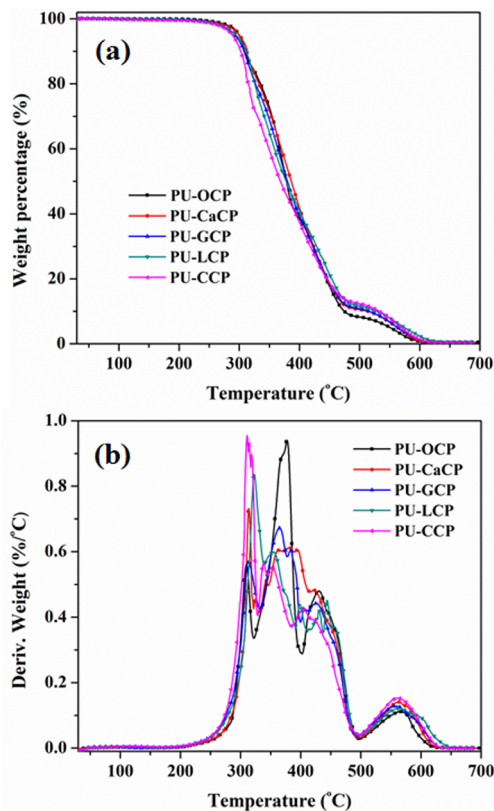


**Figure 3.** (a) TGA curves, and (b) TGA derivative curves of PUs from OCP, CaCP, GCP, LCP, and CCP.

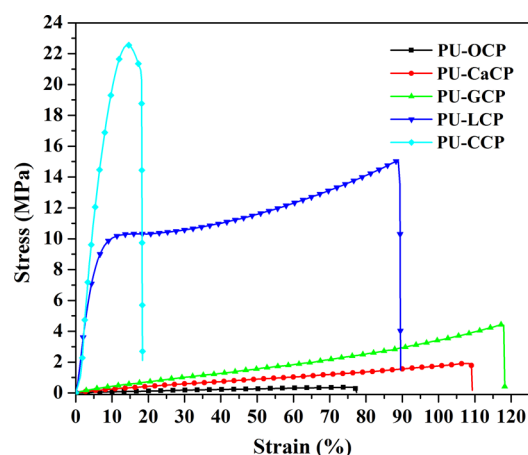


**Figure 4.** Stress–strain curves of PUs from OCP, CaCP, GCP, LCP, and CCP.

**Table 4. Mechanical Properties of PUs Based on Polyols from Different Vegetable Oils**

	tensile strength (MPa)	Young's modulus <sup>a</sup> (MPa)	elongation at break (%)	toughness (MPa)
PU-OCP	0.4 ± 0.1	0.8 ± 0.1	79.2 ± 7.1	0.16
PU-CaCP	1.7 ± 0.4	2.2 ± 0.2	96.7 ± 15.6	1.06
PU-GCP	3.7 ± 0.6	5.5 ± 0.7	96.8 ± 17.7	2.33
PU-LCP	17.3 ± 3	197.3 ± 6.2	98.0 ± 12.9	10.15
PU-CCP	29.1 ± 4	495.3 ± 41.9	11.0 ± 0.2	2.84

<sup>a</sup>Modulus calculated from the initial slope of the stress–strain curve.

elongation at break of all PUs ranged from 80 to 120%, which was attributed to the fact that the functional groups were located in the middle of the fatty acid chains, leading to a high number of dangling chains in the respective polyols.

Cyclic thermomechanical tensile tests were used to study the thermally induced shape memory effect (SME) for different vegetable oil-based PUs. Before the cyclic tests, the samples were stretched to  $\epsilon_m = 100\%$  at  $T_{\text{prog}} = T_g + 10^\circ\text{C}$  and rapidly cooled down to  $T_{\text{low}}$  ( $T_{\text{low}}$  was at least  $20^\circ\text{C}$  lower than the  $T_g$  of each sample) under an applied stress to induce the

temporary shape. Vegetable oil-based PU films are thermosets and their chemical cross-links act as permanent net points, determining the permanent shape. The shape recovery was recorded as a function of temperature by heating the samples at a rate of  $3^\circ\text{C}/\text{min}$  to  $T_{\text{high}} = T_{\text{prog}} + 10^\circ\text{C}$ . The cyclic thermomechanical tests were investigated under stress controlled conditions ( $\sigma = 0$  MPa). So that the SME could be quantified by determination of rate of recovery,  $R_r$ , and rate of fixity,  $R_f$ , from the  $\epsilon$  versus time recovery curve.

Figure 5a shows a typical thermomechanical tensile test for GCP-based PUs under stress-controlled conditions for the first cycle. The thermomechanical tensile test was repeated four times ( $N = 4$ ) under identical conditions. The value of  $R_f$  and  $R_r$  can be calculated from the deformation in the temporary shape  $\epsilon_u$  (N) and the extension at the stress free state after recovery  $\epsilon_p$  (N) according to the following equation.<sup>34</sup>

$$R_f = \epsilon_u(N)/\epsilon_m \quad (3)$$

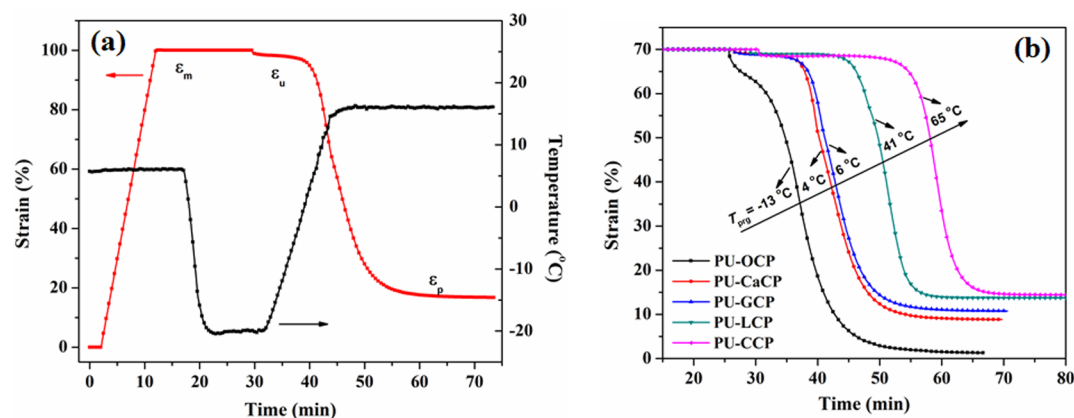
$$R_r = [\epsilon_u(N) - \epsilon_p(N)]/\epsilon_p(N) \quad (4)$$

Table 5 shows that  $R_f$  remains at approximately 98.5% independent of the number of thermomechanical test cycles. However, the value of  $R_r$  decreased from 83% for the first cycle to 79.8% for the fourth cycle.

Figure 5b shows the time dependence of strain under stress-controlled conditions for different vegetable oil-based PUs. The rate of fixity for all vegetable oil-based PU samples was approximately 98%, with the exception of PU-OCP, for which  $R_f$  was approximately 93%. This experimental result was attributed to the fact that PU-OCP's  $T_{\text{low}}$  ( $-30^\circ\text{C}$ ) was only  $20^\circ\text{C}$  lower than its  $T_{\text{prog}}$  (see Table 6). The value of  $R_r$  decreased systematically from OCP-based PU (98.19%) to CCP-based PU (78.97%) because of the difference in cross-linking density, as already mentioned.

#### 4. CONCLUSIONS

Biopolyols with different functionalities were prepared from olive, canola, grape seed, linseed, and castor oil using a solvent/catalyst-free method. Polyurethanes from these polyols were successfully prepared and characterized. The polyols from castor oil had the highest OH numbers, whereas polyols from olive oil had the lowest minimum OH number. Increasing OH numbers of the polyols resulted in an increase in cross-linking densities of the resulting PUs, leading to increasing  $T_g$  values,



**Figure 5.** (a) Strain curves of GCP-based PUs as a function of time under stress-controlled condition for the first cycle, (b) time dependence of strain under stress-controlled condition for different vegetable-oil-based PUs.



Table 5. Shape Memory Properties of GCP-Based PUs

	1st cycle		2nd cycle		3rd cycle		4th cycle	
	R <sub>f</sub> (%)	R <sub>r</sub> (%)	R <sub>f</sub> (%)	R <sub>r</sub> (%)	R <sub>f</sub> (%)	R <sub>r</sub> (%)	R <sub>f</sub> (%)	R <sub>r</sub> (%)
PU-GCP	98.46%	83.00%	98.49%	81.70%	98.47%	80.13%	98.45%	79.76%

$T_{\text{prg}} = 6\text{ }^{\circ}\text{C}$ ,  $T_{\text{low}} = -20\text{ }^{\circ}\text{C}$ ,  $T_{\text{high}} = 16\text{ }^{\circ}\text{C}$ ,  $\epsilon_m = 100\%$

Table 6. Shape Memory Properties of Different Vegetable Oil-Based PUs

	$T_{\text{g-DSC}+10}^{\text{prog}} (\text{ }^{\circ}\text{C})$	$T_{\text{low}} (\text{ }^{\circ}\text{C})$	$T_{\text{high}} = T_{\text{g-DSC}} + 20 (\text{ }^{\circ}\text{C})$	R <sub>f</sub> (%)	R <sub>r</sub> (%)
PU-OCP	-13	-30	-3	92.76	98.19
PU-CaCP	4	-20	14	98.74	87.22
PU-GCP	6	-20	16	98.47	84.39
PU-LCP	41	-10	51	98.59	80.10
PU-CCP	65	0	75	97.92	78.97

$\epsilon_m = 70\%$

Young's modulus, and tensile strength. The value of R<sub>r</sub> decreased systematically from OCP-based PUs (98.19%) to CCP-based PUs (78.97%) because of the difference in their cross-linking densities.

## ■ ASSOCIATED CONTENT

### Supporting Information

<sup>1</sup>H NMR spectra of canola oil, epoxidized canola oil, CaCP, epoxidized linseed oil, and LCP. This material is available free of charge via the Internet at <http://pubs.acs.org/>

## ■ AUTHOR INFORMATION

### Corresponding Author

\*E-mail: MichaelR.Kessler@wsu.edu.

### Notes

The authors declare no competing financial interest.

## ■ ACKNOWLEDGMENTS

This work was sponsored by Kumho Petrochemical Co. The authors give special thanks to Mengguo Yan from the Department of Chemical and Biological Engineering at Iowa State University for her valuable discussions and suggestions.

## ■ REFERENCES

- Petrovic, Z. S. Polyurethanes from Vegetable Oils. *Polym. Rev.* **2008**, *48*, 109–155.
- Kurimoto, Y.; Takeda, M.; Doi, S.; Tamura, Y.; Ono, H. Network Structures and Thermal Properties of Polyurethane Films Prepared from Liquefied Wood. *Bioresour. Technol.* **2001**, *77*, 33–40.
- Xia, Y.; Larock, R. C. Vegetable Oil-based Polymeric Materials: Synthesis, Properties, and Applications. *Green Chem.* **2010**, *12*, 1893–1909.
- Nohra, B.; Candy, L.; Blanco, J. F.; Guerin, C.; Raoul, Y.; Mouloungui, Z. From Petrochemical Polyurethanes to Biobased Polyhydroxyurethanes. *Macromolecules* **2013**, *46*, 3771–3792.
- Pfister, D. P.; Xia, Y.; Larock, R. C. Recent Advances in Vegetable Oil-Based Polyurethanes. *ChemSusChem* **2011**, *4*, 703–717.
- Ionescu, M. *Chemistry and Technology of Polyols for Polyurethanes*; Rapra Technology: Shropshire, U.K., 2005; p xvi.
- Gandini, A. Polymers from Renewable Resources: A Challenge for the Future of Macromolecular Materials. *Macromolecules* **2008**, *41*, 9491–9504.

(8) Tanaka, R.; Hirose, S.; Hatakeyama, H. Preparation and Characterization of Polyurethane Foams Using a Palm Oil-based Polyol. *Bioresour. Technol.* **2008**, *99*, 3810–3816.

(9) Luo, X. L.; Hu, S. J.; Zhang, X.; Li, Y. B. Thermochemical Conversion of Crude Glycerol to Biopolyols for the Production of Polyurethane Foams. *Bioresour. Technol.* **2013**, *139*, 323–329.

(10) Zhang, C. Q.; Ding, R.; Kessler, M. R. Reduction of Epoxidized Vegetable Oils: A Novel Method to Prepare Bio-Based Polyols for Polyurethanes. *Macromol. Rapid Commun.* **2014**, *35* (11), 1068–1074.

(11) Guo, A.; Cho, Y. J.; Petrovic, Z. S. Structure and Properties of Halogenated and Nonhalogenated Soy-based Polyols. *J. Polym. Sci. Pol Chem.* **2000**, *38*, 3900–3910.

(12) Pan, X.; Webster, D. C. New Biobased High Functionality Polyols and Their Use in Polyurethane Coatings. *ChemSusChem* **2012**, *5*, 419–429.

(13) Miao, S. D.; Zhang, S. P.; Su, Z. G.; Wang, P. Synthesis of Bio-based Polyurethanes from Epoxidized Soybean Oil and Isopropanol-amine. *J. Appl. Polym. Sci.* **2013**, *127*, 1929–1936.

(14) Kiatsimkul, P. P.; Suppes, G. J.; Hsieh, F. H.; Lozada, Z.; Tu, Y. C. Preparation of High Hydroxyl Equivalent Weight Polyols from Vegetable Oils. *Ind. Crop Prod* **2008**, *27*, 257–264.

(15) Zhang, C. Q.; Xia, Y.; Chen, R. Q.; Huh, S.; Johnston, P. A.; Kessler, M. R. Soy-Castor Oil based Polyols Prepared Using a Solvent-free and Catalyst-free Method and Polyurethanes Therefrom. *Green Chem.* **2013**, *15*, 1477–1484.

(16) Lu, Y. S.; Larock, R. C. Soybean-Oil-Based Waterborne Polyurethane Dispersions: Effects of Polyol Functionality and Hard Segment Content on Properties. *Biomacromolecules* **2008**, *9*, 3332–3340.

(17) Petrovic, Z. S.; Zhang, W.; Zlatanic, A.; Lava, C. C.; Ilavsky, M. Effect of OH/NCO Molar Ratio on Properties of Soy-based Polyurethane Networks. *J. Polym. Environ* **2002**, *10*, 5–12.

(18) Peruzzo, P. J.; Anbinder, P. S.; Pardini, O. R.; Vega, J. R.; Amalvy, J. I. Influence of Diisocyanate Structure on the Morphology and Properties of Waterborne Polyurethane-Acrylates. *Polym. J.* **2012**, *44*, 232–239.

(19) del Rio, E.; Lligadas, G.; Ronda, J. C.; Galia, M.; Meier, M. A. R.; Cadiz, V. Polyurethanes from Polyols Obtained by ADMET Polymerization of a Castor Oil-Based Diene: Characterization and Shape Memory Properties. *J. Polym. Sci. Pol Chem.* **2011**, *49*, 518–525.

(20) Khot, S. N.; Lascala, J. J.; Can, E.; Morye, S. S.; Williams, G. L.; Palmese, G. R.; Kusefoglu, S. H.; Wool, R. P. Development and Application of Triglyceride-based Polymers and Composites. *J. Appl. Polym. Sci.* **2001**, *82*, 703–723.

(21) Mutlu, H.; Meier, M. A. R. Castor Oil as a Renewable Resource for the Chemical Industry. *Eur. J. Lipid Sci. Tech* **2010**, *112*, 10–30.

(22) Ogunniyi, D. S. Castor oil: Vital Industrial Raw Material. *Bioresour. Technol.* **2006**, *97*, 1086–1091.

(23) Dworakowska, S.; Bogdal, D.; Prociak, A. Microwave-Assisted Synthesis of Polyols from Rapeseed Oil and Properties of Flexible Polyurethane Foams. *Polymers-Basel* **2012**, *4*, 1462–1477.

(24) Dai, H. H.; Yang, L. T.; Lin, B.; Wang, C. S.; Shi, G. Synthesis and Characterization of the Different Soy-Based Polyols by Ring Opening of Epoxidized Soybean Oil with Methanol, 1,2-Ethanediol and 1,2-Propanediol. *J. Am. Oil Chem. Soc.* **2009**, *86*, 261–267.

(25) Kong, X. H.; Liu, G. G.; Qi, H.; Curtis, J. M. Preparation and Characterization of High-Solid Polyurethane Coating Systems Based on Vegetable Oil Derived Polyols. *Prog. Org. Coat.* **2013**, *76*, 1151–1160.

- (26) Javni, I.; Hong, D. P.; Petrovic, Z. S. Polyurethanes from Soybean Oil, Aromatic, and Cycloaliphatic Diamines by Non-Isocyanate Route. *J. Appl. Polym. Sci.* **2013**, *128*, 566–571.
- (27) Andjelkovic, D. D.; Valverde, M.; Henna, P.; Li, F. K.; Larock, R. C. Novel Thermosets Prepared by Cationic Copolymerization of Various Vegetable Oils - Synthesis and Their Structure-Property Relationships. *Polymer* **2005**, *46*, 9674–9685.
- (28) Lu, Y. S.; Larock, R. C. Soybean Oil-based, Aqueous Cationic Polyurethane Dispersions: Synthesis and Properties. *Prog. Org. Coat.* **2010**, *69*, 31–37.
- (29) Petrovic, Z. S.; Yang, L. T.; Zlatanic, A.; Zhang, W.; Javni, I. Network Structure and Properties of Polyurethanes from Soybean Oil. *J. Appl. Polym. Sci.* **2007**, *105*, 2717–2727.
- (30) Zlatanic, A.; Lava, C.; Zhang, W.; Petrovic, Z. S. Effect of Structure on Properties of Polyols and Polyurethanes Based on Different Vegetable Oils. *J. Polym. Sci. Pol Phys.* **2004**, *42*, 809–819.
- (31) Javni, I.; Petrovic, Z. S.; Guo, A.; Fuller, R. Thermal Stability of Polyurethanes Based on Vegetable Oils. *J. Appl. Polym. Sci.* **2000**, *77*, 1723–1734.
- (32) Gaboriaud, F.; Vantelon, J. P. Mechanism of Thermal-Degradation of Polyurethane Based on Mdi and Propoxylated Trimethylol Propane. *J. Polym. Sci. Pol Chem.* **1982**, *20*, 2063–2071.
- (33) Xia, Y.; Larock, R. C. Castor-Oil-Based Waterborne Polyurethane Dispersions Cured with an Aziridine-Based Crosslinker. *Macromol. Mater. Eng.* **2011**, *296*, 703–709.
- (34) Miao, S. D.; Callow, N.; Wang, P.; Liu, Y. Y.; Su, Z. G.; Zhang, S. P. Soybean Oil-Based Polyurethane Networks: Shape-Memory Effects and Surface Morphologies. *J. Am. Oil Chem. Soc.* **2013**, *90*, 1415–1421.